# Evaluation of Dose Distribution at the Level of Electronic Portal Imaging Device using Treatment Planning System

Amene Bagheri (MSc)[1], Mehdi Momennezhad (PhD)[2], Shahrokh Nasseri (PhD)[3], Azam Eskandari (PhD Candidate)[1], Erfan Saatchian (PhD Candidate)[1], Maryam Naji (MSc)[1], Mohammad Yasin Mohammadi (PhD)[1]*

[1]Department of Medical Physics, Mashhad University of Medical Sciences, Mashhad, Iran
[2]Nuclear Medicine Research Center, Mashhad University of Medical Sciences, Mashhad, Iran
[3]Medical Physics Research Center, Mashhad University of Medical Sciences, Mashhad, Iran

## ABSTRACT

**Background:** Treatment Planning Systems (TPS) are designed to calculate dose distributions within the CT imaging field of view. However, the Electronic Portal Imaging Device (EPID) is positioned outside this area, making it challenging to use standard TPS for dose calculations at the EPID level.

**Objective:** The objective of this study is to present an innovative approach to address the limitations of TPS in calculating dose distribution at the EPID level.

**Material and Methods:** In this retrospective quantitative study, the CT image was extended to the EPID level and imported into the TPS. 42 treatments were planned, and doses were calculated. The TPS doses were then compared with the measured doses obtained using an Ion Chamber (IC). The study also investigated the impact of field size, phantom thickness, and air gap for energies of 6, 10, and 15 MV.

**Results:** The average, minimum, and maximum dose differences were 1.91%, 0.02%, and 5.79% when changing the field size from 5×5 $cm^2$ to 20×20 $cm^2$, 3.62%, 0.18%, and 6.91% when the phantom thickness changed from 10 to 30 cm, and 3.5%, 0.4%, and 7.46% when the air gap was varied from 30 to 60 cm respectively. 97% of all changes in IC values can be predicted through the linear relationship with TPS.

**Conclusion:** The validated proposed method in this study, as an innovative approach, effectively addresses the limitation of TPS in calculating dose distribution at the EPID level. This can be used as a reference for comparing the measured dose obtained by EPID in dosimetric verification.

## Keywords

Radiotherapy; Radiotherapy Setup Errors; Radiation Dosimetry; Electronic Portal Imaging Device; Treatment Planning System

## Introduction

One of the primary challenges in radiotherapy is ensuring the accurate delivery of the prescribed dose to the treatment target. Despite significant advancements in radiation therapy techniques, the potential for errors in dose delivery persists. Therefore, ensuring quality assurance and treatment verification is crucial to achieve high accuracy in dose delivery and to provide appropriate patient care [1-3]. Dosimetric verification plays a critical role in the final

*Corresponding author:
Mohammad Yasin Mohammadi
Department of Medical Physics, Mashhad University of Medical Sciences, Mashhad, Iran
E-mail: mohammadimy2@mums.ac.ir

Received: 28 December 2023
Accepted: 26 May 2024

confirmation of treatment, aiming to validate the accurate delivery of the prescribed dose to the patient. In this process, the dose is measured using a detector before and during treatment, and then compared to the dose prescribed in the treatment plan generated by the Treatment Planning System (TPS) [4-6].

The Electronic Portal Imaging Device (EPID) is utilized as an effective method for verifying the geometric positioning of patients and is commonly used in dosimetric verification [7-11]. Dosimetric verification with EPID involves two distinct approaches:

1) Transmitted and non-transmitted dosimetry methods:

- Non-transmitted dosimetry: In this approach, there is no attenuating substance between the radiation source and the detector. This technique is appropriate for ensuring quality control [12,13].

- Transmitted dosimetry: With this method, the radiation penetrates through the patient (or phantom) and reaches the detector. It is valuable for detecting errors associated with the machine and patient, such as variations in tumor dimensions, patient weight, and internal organ movement [14,15].

2) Forward and back projection:

- Forward Projection: The comparison between the measured Portal Dose Images (mPDIs) acquired with a calibrated EPID and the predicted Portal Dose Images (pPDIs) at the EPID location is conducted to evaluate the accuracy of dose delivery [16,17].

- Back Projection: The measured dose distribution captured with the calibrated EPID is projected back to a specific depth within the patient's body or phantom using back projection reconstruction techniques [18-20].

In the Forward Projection method, the dose distribution measured at the EPID location is juxtaposed with the measured dose distribution derived from the reference EPID. On the other hand, the Back Projection technique involves comparing the measured dose distribution within the patient's body or phantom with the predicted dose distribution computed by the TPS [21-23].

Using the Forward Projection method for dosimetric verification poses challenges when comparing the mPDI with the dose calculated by the TPS at the EPID level. The TPS conducts dose calculations within the CT imaging field of view. Given that the EPID is positioned at a distance varying from 60-40 cm from the isocenter and 140-160 cm from the radiation source, and is outside the CT imaging field of view, utilizing TPS for dose distribution calculation at the EPID location is difficult and comes with limitations. Obtaining the calculated dose distribution at the EPID level using standard TPS tools is not feasible.

In this study, an innovative approach was used to overcome the limitations and perform dosimetric verification at the EPID level using the Forward Projection method, which has less complexity compared to Back Projection. Therefore, the proposed method can provide a faster and more accurate approach for dosimetric verification by comparing the measured EPID dose distribution with the calculated predicted TPS dose distribution as a reference at the EPID level. Moreover, this method can be employed for quality control in the radiotherapy department.

## Material and Methods

### Image processing

This is a phantom-based study. The phantoms were imaged using a Hitachi Superia CT machine at 120 kVp, with a 512×512 matrix size and a 5 mm slice thickness. The CT images of a water slab phantom were brought into the IsoGray treatment planning system (DosiSoft® France). The isocenter and radiation fields were established at the specified angle. The RTPlan file, containing beam data and isocenter point coordinates, was extracted and subsequently imported into 3Dslicer (version 4.11.0) [24]. The steps of image processing of CT image in the 3D slicer are summarized (as

shown in Figure 1):

A: The CT image and RTPlan file were imported into the 3D slicer. B: Because the coordinate system definitions in the RTPlan file (in DICOM format) and the 3D slicer differ, adjustments are necessary, including modifying the gantry angle and jaw positions for rectangular fields. All measurements are specified in the anterior-posterior (AP) projection. C: The isocenter point is loaded in 3D Slicer. D: The EPID model was defined as a rectangular cube with dimensions of 41×41×5 $cm^3$. E: according to the coordinates of the isocenter point and the gantry angle, a point as the center of EPID was placed in the correct coordinates. F: The transfer module was used to move the EPID model, defined in step D, to the coordinates of the EPID center point. It was then rotated in the correct direction based on the gantry angle. G: The CT image was enlarged to fully encapsulate the EPID model. Air CT number (-1000 HU) was assigned to the added pixels. H: The EPID was transformed from model mode to volume mode, where CT numbers can be assigned to the EPID. This step created a distinct EPID image separate from the CT image. I: The EPID model image was temporarily assigned a CT number of 1000 HU, while the areas outside the EPID model were assigned a CT number of 0 HU. J: To combine two

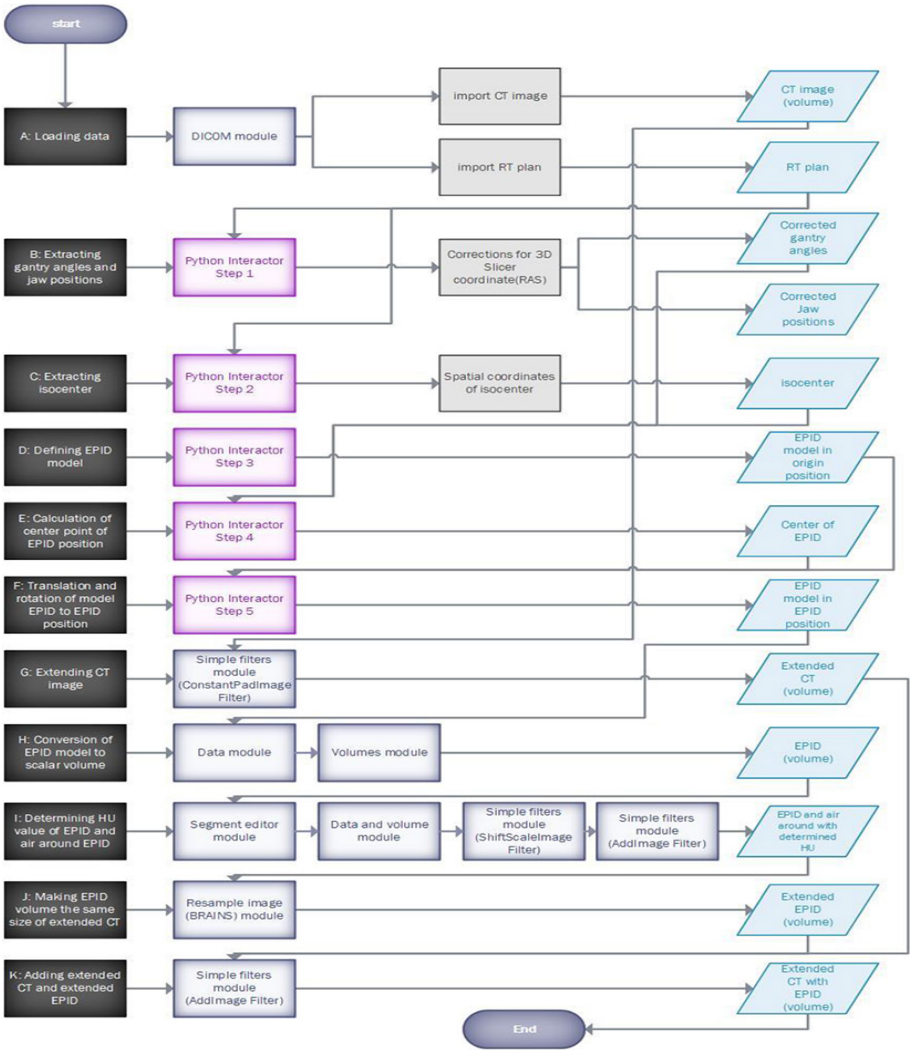


**Figure 1:** Image processing steps in 3D slicer

images, they must have identical dimensions. Thus, the EPID image was resized to match the dimensions of the CT image. K: In the end, two images were combined, resulting in a new CT image that accurately positions the patient phantom and EPID model (as shown in Figure 2a). During EPID dosimetry, the EPID-captured image is transformed into a dose distribution in water, with pixels of the EPID model assigned to the CT number of water (0 HU). Additionally, for the other pixels added, the CT number of air (-1000 HU) was assigned.

## Treatment planning and dose calculations

The images from the previous step were imported into the TPS. 42 planes were utilized to analyze the impact of field size, air gap size (the distance between the lowest part of the patient phantom and the surface of the EPID phantom), and phantom thickness at three different energies (6, 10, and 15 MV) on the calculated dose by TPS, as shown in Figure 2a, and Table 1. In these plans, the surface of the EPID model is positioned at a constant distance of 160 cm from the radiation source. To validate the dosimetry results calculated by the TPS, it is essential to compare them with the dosimetry measurement (as shown in Figure 2b).

## Ion chamber dose measurements

The dose measurement is performed by an ionization chamber (IC) of the Farmer type (PTW) with a volume of 0.6 $cm^3$, which serves as the gold standard. To achieve this, we set up the following arrangement as depicted in Figure 2b. In this setup, we place 20 water-equivalent phantoms, each measuring 30 cm in length and width and 1 cm in thickness, on the treatment couch to serve as the patient phantom. An additional 25 slab phantoms are positioned as EPID phantoms at the EPID level. Throughout The ionization chamber dosimeter is inserted into one of the perforated slabs at the appropriate depth along the central axis of the beam. Due to the build-up effect and the dependence of the maximum dose depth on energy, selecting the appropriate measurement depth is crucial. In this study, the depth of measurement selected is 2 cm, according to a similar study [25]. Following precise setup, radiation is administered using the Elekta linear accelerator machine type precise in Imam Reza Hospital, matching the TPS plans in terms of specific energy, field size, phantom thickness, and air gap, and the dose is

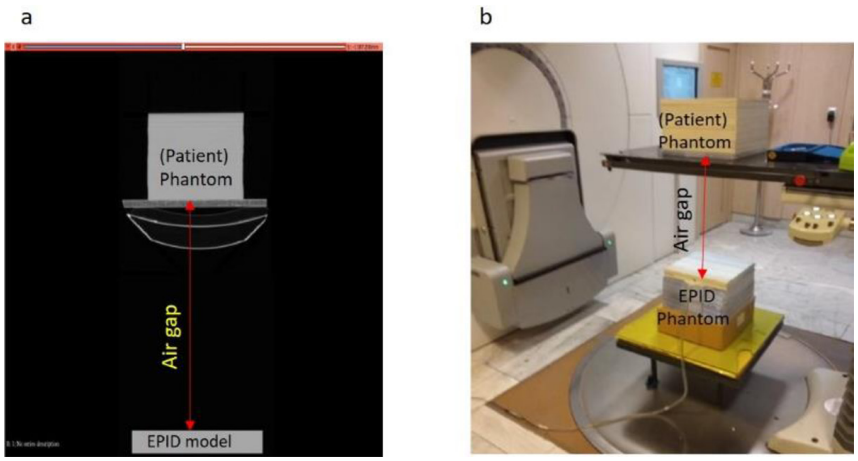


**Figure 2:** **a**) The setup of the patient phantom, the Electronic Portal Imaging Device (EPID) model, and air gap in Treatment Planning Systems (TPS). **b**) The setup of the patient phantom, EPID phantom, and air gap in the treatment room.

**Table 1:** Variable parameters to evaluate dose calculations of treatment planning systems (TPS)

| Energy (MV) | 6,10,15 |
|---|---|
| Phantom thickness (cm) | 10,20,30 |
| Field size ($cm^2$) | 5×5, 10×10, 20×20 |
| Air gap (cm) | 30, 40, 50,60 |

measured.

### Determination of the dose calculation depth

The optimal TPS dose calculation depth in the EPID model should correspond to the IC dose measurement depth in the EPID phantom. To find this point, dose calculations for depths ranging from 1 to 5 cm in the EPID model are conducted for field sizes ranging from 5×5 $cm^2$ to 20×20 $cm^2$, with energies of 6, 10, and 15 MV, SSD of 90 cm, a patient phantom thickness of 20 cm, and a fixed air gap of 50 cm using the TPS, normalized to the standard field size (10×10 $cm^2$). By comparing the results calculated by the TPS with the results obtained from ionization chamber measurements under similar radiation conditions from the EPID phantom, the most suitable measurement depth is determined. It can be concluded that this selected depth of the EPID phantom corresponds to the depth of the EPID model in the TPS where the dose calculation and measurement are performed at the same depth.

### Relative dose comparison

After identifying the suitable point, the dose evaluation will be conducted solely at this location to investigate the impact of field size, patient phantom thickness, and air gap parameters at different energies by comparing the TPS-calculated dose with the IC-measured dose.

#### Field size

Variations in field size result in alterations in scatter, thus causing the dose response along the central axis to be influenced by the field size. The effect of field size, in the presence of an attenuating material (patient phantom), is being investigated using field sizes ranging from 5×5 $cm^2$ to 20×20 $cm^2$ for three energies, with an SSD of 90 cm, a phantom thickness of 20 cm, and a fixed air gap of 50 cm. The TPS dose calculations will be compared with the IC measurements in similar radiation conditions.

#### Patient Phantom thickness

Variations in phantom thickness can influence scattering, absorption patterns, and energy spectrum. The impact of phantom thickness is investigated using phantoms of 10, 20, and 30 cm for three energies, with a fixed field size of 10×10 $cm^2$. TPS dose calculations will be compared with IC measurements under similar radiation conditions. The assessment is conducted through two distinct methods. In the first case, only variations in phantom thickness are considered, with a fixed air gap of 60 cm. As a result, the SSD for phantoms of 10, 20, and 30 cm in thickness is 90, 80, and 70 cm, respectively. In the second case (SAD treatment), changes in both phantom thickness and the air gap are taken into account. For phantoms of 10, 20, and 30 cm in thickness, the air gap is 55, 50, and 45 cm, and the SSD is 95, 90, and 85 cm, respectively. In this scenario, the isocenter point for all measurements is positioned at the center of the phantom.

#### Air gap

The transmitted beam comprises both primary photons and scattered photons from the phantom. Altering the air gap dimensions changes the ratio of scattered to primary photons. Therefore, the variation of this parameter should also be studied. The effect of air gap sizes of 30, 40, 50, and 60 cm is investigated for all three energies, with a field size of 10×10 $cm^2$, a phantom thickness of 20 cm, and SSD of 110, 100, 90, and 80 cm, respectively. The TPS dose calculations will be compared with the IC measurements under similar radiation conditions.

### Absolute dose comparison

The absolute dose calculated by TPS and the absolute dose measured by IC are compared (without normalizing to the reference point). In this comparison, the independent investigation of field size, phantom thickness, and air gap size allows us to determine the level of agreement between the dose calculated by TPS and the dose measured by IC using this analysis.

### Equation between the measured dose and the calculated dose

To determine the optimal equation between the calculated and measured values, a scatter plot was created, depicting the IC values against the TPS values for all 42 cases. By examining this plot, it is possible to identify the linear variation of IC, as defined by the linear relationship between IC and TPS.

## Results

### Selecting the best measurement depth

Figure 3 ( a, b, and c) depicts the comparison between TPS dose calculations at depths ranging from 1 to 5 cm of the EPID model for three energies and various field sizes, with IC dose measurements of the EPID phantom. The

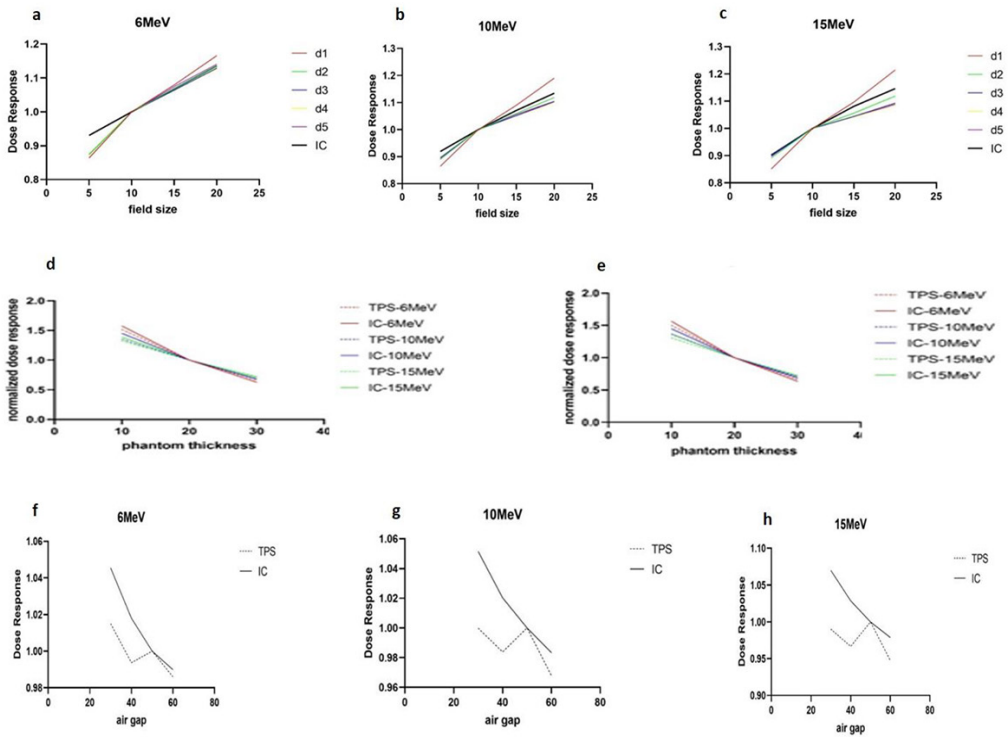


**Figure 3:** (**a, b, c**) The correlation between field size and the normalized dose response, calculated by Treatment Planning Systems (TPS) and measured by the Ion Chamber (IC) for different energies, additionally, the comparison between TPS dose calculations at depths ranging from 1 to 5 cm of the Electronic Portal Imaging Device (EPID) model, with IC dose measurements of the EPID phantom.
(**d, e**) The correlation between patient phantom thickness and the normalized dose response, calculated by TPS and measured by the IC for different energies d) fixed air gap of 60 cm and e) various air gaps at 55, 50, and 45 cm. (**f, g, h**) The correlation between air gap size and the normalized dose response was calculated by TPS and measured by the IC for different energies.

results were normalized to a field size of 10×10 $cm^2$. The horizontal axis represents the size of one side of the square field at the isocenter, while the vertical axis represents the normalized dose response. The closest agreement was observed at a depth of 2 cm. This indicates that a depth of 2 cm from the EPID model in the TPS corresponds to practical measurements obtained from the IC at a depth of 2 cm from the EPID phantom. Subsequent calculations will therefore utilize data related to this depth. The maximum discrepancies between TPS and IC values were observed for small field sizes. However, these errors decreased for higher energies.

## Relative dose comparison

### Field size

Figure 3 (a, b, and c) illustrates the correlation between field size and the normalized dose response, calculated by TPS and measured by the IC for different energies. The results were normalized to a field size of 10×10 $cm^2$. The horizontal axis represents the size of one side of the square field at the isocenter, while the vertical axis represents the normalized dose response. For all energies (6, 10, and 15 MV), an increase in field size increased the dose response in IC and TPS values. The TPS-calculated dose was compared to the IC-measured dose. The maximum dose difference is 5.97% for 6 MV energy and 5×5 a $cm^2$ field size. The minimum dose difference is 0.02% for 6 MV energy and 20×20 $cm^2$ field size. The average dose difference for 6, 10, and 15 MV energies are 2.1%, 1.77%, and 1.96% respectively.

### Patient Phantom thickness

Figure 3 (d,e) demonstrates the correlation between phantom thickness and the normalized dose response, calculated by TPS and measured by the IC for different energies. The values are normalized based on a phantom thickness of 20 cm. The horizontal axis represents the phantom thickness, while the vertical axis represents the normalized dose response. Figure 3d pertains to the fixed air gap of 60 cm, while Figure 3e relates to variable air gaps of 55 cm, 50 cm, and 45 cm. As expected, there is an exponential decrease in the dose response as the phantom thickness increases. For higher energies, the slope of the curve becomes less steep. The TPS-calculated dose was compared to the IC-measured dose. The maximum dose difference between TPS dose calculations and IC dose measurements is 6.91%, occurring with a phantom thickness of 10 cm for an energy of 10 MV. Conversely, the minimum dose difference is 0.18%, observed with a phantom thickness of 30 cm for an energy of 15 MV. The average dose differences for setup a (fixed air gap) are 4.41%, 3.83%, and 2.9% for energies of 6, 10, and 15 MV, respectively. On the other hand, the average dose differences for setup b (various air gaps) are 4.35%, 4.07%, and 2.18% for energies of 6, 10, and 15 MV, respectively.

### Air gap

Figure 3 (f, g, and h) depicts the relationship between air gap size and normalized dose response, as calculated by TPS and measured by the IC for various energies. The values are normalized based on an air gap size of 50cm. The horizontal axis represents the air gap size, while the vertical axis represents the normalized dose response. The IC response curve shows a decrease in dose as the air gap size increases. It is expected that the TPS calculation would exhibit a decreasing trend in the dose and air gap relationship compared to the IC measurements. However, an increase in the dose is observed at a specific point of the air gap (50 cm). The TPS-calculated dose was compared to the IC-measured dose. The maximum dose difference between the TPS-calculated dose and the IC-measured dose is 7.46%, occurring with an energy of 15 MV and an air gap size of 30 cm. Conversely, the minimum dose difference is 0.04%, observed with an energy of 6 MV and an air gap size of 60 cm. The average dose differences for energies of 6, 10, and 15 MV are 1.9%, 3.3%, and 5.5% respectively. It's important to note that

the percentage differences in dose are influenced by inaccuracies in the TPS calculations.

### Absolute dose comparison

Figure 4 depicts the comparison between the absolute dose calculated by TPS and the absolute dose measured by IC for various field sizes, phantom thicknesses, and air gap sizes, considering three different energies. According to Figure 4, TPS overestimates 3±0.73 cGy on average.

### Equation between the measured dose and the calculated dose

Figure 5 shows a scatter plot for IC measurements and TPS calculations. The regression line equation is:

Eq: IC=(0.969×TPS)–2.385

The coefficient of determination for the regression line is 0.967, which shows that 97% of IC changes are determined through the linear relationship between IC and TPS.

## Discussion

### Depth of dose measurement and calculation

The dose calculation point obtained in this study, at the depth of 2 cm of the EPID model, was in good agreement with IC measurements for energies of 6, 10, and 15 MV. Saboori compared IC measurements with values calculated

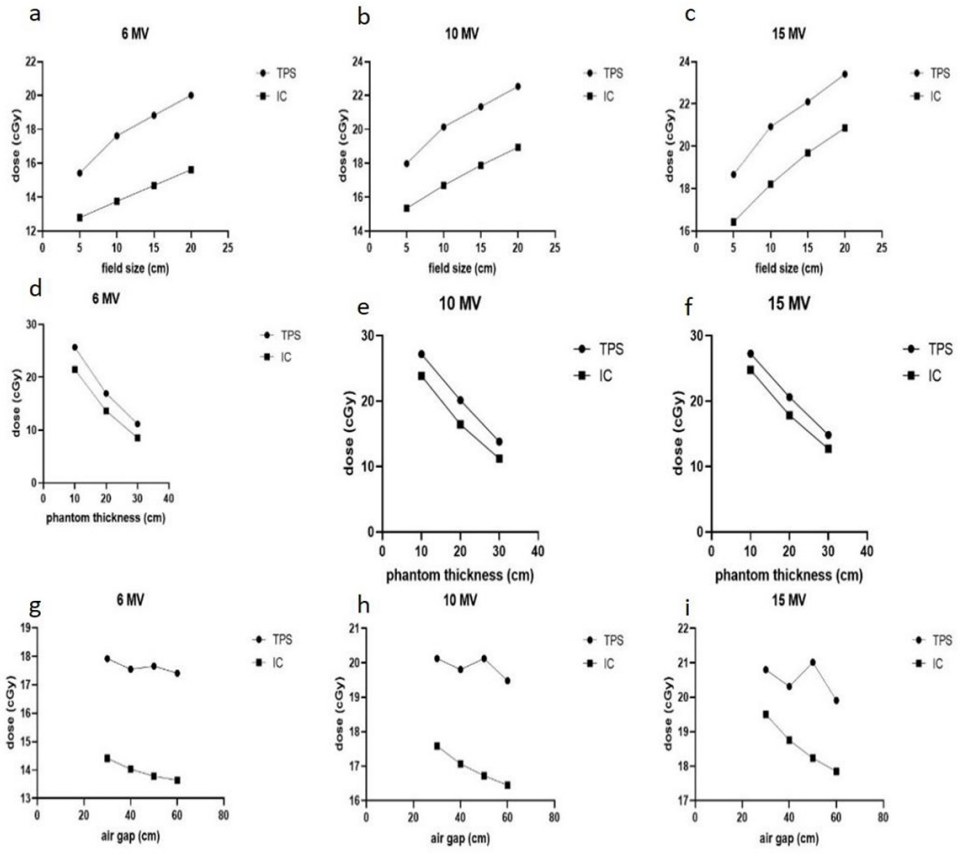


**Figure 4:** The comparison between the absolute dose calculated by Treatment Planning Systems (TPS) and the absolute dose measured by Ion Chamber (IC) includes various aspects: **a-c**) Field size variation **d-f**) Phantom thickness variation **g-i**) Air gap size variation. These variations are considered for three different energies.

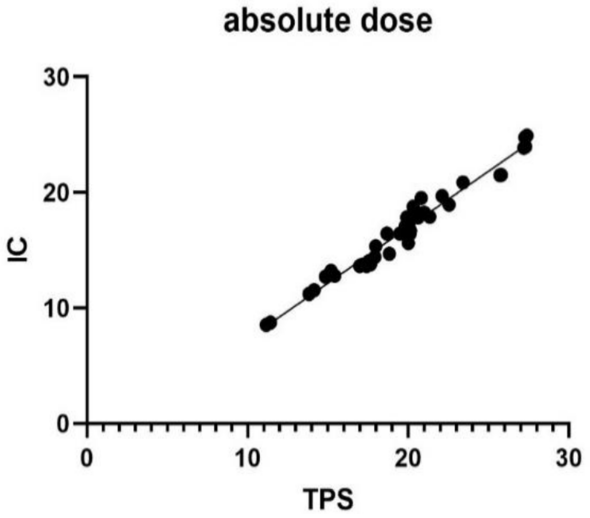


**Figure 5:** The scatter plot for Ion Chamber (IC) measurements and Treatment Planning Systems (TPS) calculations

for different depths of the EPID model and reported that the calculated values at a depth of 2 cm have the closest similarity to the measured values for energies of 6 and 15 MV [25]. For the energy of 6 MV, Reich et al. used a depth of 1.5 cm of the EPID model to compare with measured results, and this depth was found to be appropriate [26]. The maximum discrepancies between TPS and IC values were observed for small field sizes, but these errors decreased for higher energies. It is worth noting that the dose calculated by TPS at a depth of 1 cm in the EPID model showed less resemblance to the IC measurements, likely due to electron equilibrium not being achieved at this depth.

## Field size

In the present study, it was observed that an increase in field size from 5×5 $cm^2$ to 20×20 $cm^2$ resulted in a corresponding increase in the dose response for all energies (6, 10, and 15 MV) in both the ionization chamber (IC) and the treatment planning system (TPS) values. The percentage difference between the TPS and the IC values ranged from 0.02% to 6%, and as the field size increased, the percentage difference decreased. These results are consistent with the study by Bertholet et al., in which the effect of field size was evaluated by changing this parameter from 6.6 cm2 to 20×20 $cm^2$, and the percentage difference ranged from 0.06% to 4.6% [27].

## Patient Phantom thickness

In the present study, an exponential reduction relationship between the phantom thickness and dose response is observed in the diagram. As the energy increases, the slope of the graph decreases. The percentage difference between the TPS and the IC values ranged from 0.02% to 6.91%. This difference decreases with increasing phantom thickness. These results are consistent with findings from other studies. In the Saboori study, it was demonstrated that as the energy increases, the effect of phantom thickness on dose response decreases (the slope of the graph decreases) because for high energies, scattering is more forward and thickness changes have less effect on dose changes [25]. In Reich's study, the maximum percentage difference related to phantom thickness was 5%, and the average percentage difference was less than 2%. They reported that the percentage difference increased with decreasing phantom thickness [26].

## Air gap

Another crucial factor to consider is the air gap size, which has not been extensively studied in previous research. As the air gap increases, the proportion of scattered beams to primary beams changes due to fewer scattered rays reaching the detector. In this study, we investigated the impact of the air gap on dose response. The TPS-calculated dose was compared to the IC-measured dose, revealing a percentage difference ranging from 0.4% to 7.46%. Consistent with the Deshpande report, an increase in the air gap leads to a decrease in the percentage difference. Deshpande's report suggests that as the air gap widens, the

percentage difference between the TPS-calculated dose and the dose measured by the calibrated EPID decreases [7]. In comparison to the IC measurements and the study by Saboori [25], a decreasing trend in the dose and air gap relationship is expected in the TPS calculation. However, an increase in the dose is observed at a specific air gap size (50 cm). This deviation might be due to the lack of clarity in dose calculations at large distances within the dose calculation algorithm. In this study, we evaluated this parameter at a few specific distances with 10 cm intervals (air gap 30, 40, 50, and 60 cm). To better understand the behavior of this parameter, it should be evaluated in smaller increments. Given the lack of precise predictions for air gap changes, this parameter needs to be independently and more precisely studied with smaller increments (e.g., 2 cm) in subsequent research.

## Conclusion

The TPS conducts dose calculations within the CT imaging field of view. However, due to the variable distances between the EPID and the isocenter and radiation source (typically 60-40 cm from the isocenter and 140-160 cm from the source), the use of TPS for dose distribution calculation at the EPID location presents challenges and limitations, as the EPID is typically positioned outside the CT imaging field of view. Obtaining the calculated dose distribution at the EPID level using standard TPS tools is difficult. Despite these limitations, TPS has the potential to calculate dose distribution at the EPID level.

In this study, the 3D Slicer software is utilized for the first time to address the limitations of TPS in dose calculation at the EPID level. The proposed method, validated in this study as an innovative approach, overcomes the limitations of TPS in calculating EPID level dose distribution. This study evaluates the accuracy of TPS dose calculation at the EPID level. The dose calculated by TPS can serve as a reference for comparison with the measured dose obtained by EPID in dosimetry verification. Additionally, this method can be utilized for quality control in the radiotherapy department.

## Authors' Contribution

M. Momennezhad and Sh. Nasseri conceived the idea. Introduction of the paper was written by MY. Mohammadi and E. Saatchian. A. Bagheri, A. Eskandari and M. Naji gather the images and the related literature and also help with writing of the related works. The method implementation was carried out by Sh.Nasseri, M. Momennezhad, MY. Mohammadi and A. Bagheri. Results and Analysis was carried out by Sh.Nasseri, M. Momennezhad and A. Bagheri. The research work was proofread and supervised by Sh. Nasseri, M. Momennezhad and MY. Mohammadi. All the authors read, modified, and approved the final version of the manuscript.

## Ethical Approval

This study was approved by the Ethics Committee of Mashhad University of Medical Sciences (IR.MUMS.MEDICAL.REC.1401.150).

## Funding

This study is a part of the PhD thesis and supported by the vice chancellor for research of Mashhad University of Medical Science (Project Number 4000754).

## Conflict of Interest

None

## References

1. Olaciregui-Ruiz I, Beddar S, Greer P, Jornet N, McCurdy B, Paiva-Fonseca G, et al. In vivo dosimetry in external beam photon radiotherapy: Requirements and future directions for research, development, and clinical practice. *Phys Imaging Radiat Oncol*. 2020;**15**:108-16. doi: 10.1016/j.phro.2020.08.003. PubMed PMID: 33458335. PubMed PMCID: PMC7807612.
2. Grządziel A, Gądek A, Bekman B, Wendykier

J, Ślosarek K. Synthetic CT in assessment of anatomical and dosimetric variations in radiotherapy-procedure validation. *Pol J Med Phys Eng*. 2020;**26**(4):185-92. doi: 10.2478/pjmpe-2020-0022.

3. Baek TS, Chung EJ, Son J, Yoon M. Feasibility study on the verification of actual beam delivery in a treatment room using EPID transit dosimetry. *Radiat Oncol.* 2014;**9**:273. doi: 10.1186/s13014-014-0273-8. PubMed PMID: 25472838. PubMed PMCID: PMC4262986.
4. Van Elmpt W, McDermott L, Nijsten S, Wendling M, Lambin P, Mijnheer B. A literature review of electronic portal imaging for radiotherapy dosimetry. *Radiother Oncol.* 2008;**88**(3):289-309. doi: 10.1016/j.radonc.2008.07.008. PubMed PMID: 18706727.
5. Kairn T, Cassidy D, Sandford PM, Fielding AL. Radiotherapy treatment verification using radiological thickness measured with an amorphous silicon electronic portal imaging device: Monte Carlo simulation and experiment. *Phys Med Biol*. 2008;**53**(14):3903-19. doi: 10.1088/0031-9155/53/14/012. PubMed PMID: 18591736.
6. Van Elmpt WJ, Nijsten SM, Dekker AL, Mijnheer BJ, Lambin P. Treatment verification in the presence of inhomogeneities using EPID-based three-dimensional dose reconstruction. *Med Phys*. 2007;**34**(7):2816-26. doi: 10.1118/1.2742778. PubMed PMID: 17821989.
7. Deshpande S, Blake SJ, Xing A, Metcalfe PE, Holloway LC, Vial P. A simple model for transit dosimetry based on a water equivalent EPID. *Med Phys.* 2018;**45**(3):1266-75. doi: 10.1002/mp.12742. PubMed PMID: 29314080.
8. Nailon WH, Welsh D, McDonald K, Burns D, Forsyth J, Cooke G, et al. EPID-based in vivo dosimetry using Dosimetry Check™: Overview and clinical experience in a 5-yr study including breast, lung, prostate, and head and neck cancer patients. *J Appl Clin Med Phys.* 2019;**20**(1):6-16. doi: 10.1002/acm2.12441. PubMed PMID: 30536528. PubMed PMCID: PMC6333145.
9. Najem MA, Tedder M, King D, Bernstein D, Trouncer R, Meehan C, Bidmead AM. In-vivo EPID dosimetry for IMRT and VMAT based on through-air predicted portal dose algorithm. *Phys Med.* 2018;**52**:143-53. doi: 10.1016/j.ejmp.2018.07.010. PubMed PMID: 30139603.
10. Ahmadi E, Eskandari A, Mohammadi M, Naji M, Naseri S, Gholamhosseinian H. Evaluation of Interfractional Setup Uncertainties and Calculation of Adequate CTV-PTV Margin for Head and Neck Radiotherapy using Electronic Portal Imaging Device. *J Biomed Phys Eng.* 2023. doi: 10.31661/jbpe.v0i0.2211-1565.
11. Hashemi SM, Bahreyni MH, Mohammadi M, Nasseri S, Bayani S, Gholamhosseinian H, et al. An Empirical Transmitted EPID Dosimetry Method using a Back-Projection Algorithm. *J Biomed Phys Eng*. 2019;**9**(5):551-8. doi: 10.31661/jbpe.v0i0.1082. PubMed PMID: 31750269. PubMed PMCID: PMC6820021.
12. Bailey DW, Kumaraswamy L, Bakhtiari M, Malhotra HK, Podgorsak MB. EPID dosimetry for pretreatment quality assurance with two commercial systems. *J Appl Clin Med Phys.* 2012;**13**(4):3736. doi: 10.1120/jacmp.v13i4.3736. PubMed PMID: 22766944. PubMed PMCID: PMC5716510.
13. Sharma DS, Mhatre V, Heigrujam M, Talapatra K, Mallik S. Portal dosimetry for pretreatment verification of IMRT plan: a comparison with 2D ion chamber array. *J Appl Clin Med Phys*. 2010;**11**(4):3268. doi: 10.1120/jacmp.v11i4.3268. PubMed PMID: 21081884. PubMed PMCID: PMC5720403.
14. Mijnheer B, Beddar S, Izewska J, Reft C. In vivo dosimetry in external beam radiotherapy. *Med Phys.* 2013;**40**(7):070903. doi: 10.1118/1.4811216. PubMed PMID: 23822404.
15. Mohammadi M, Bezak E. Evaluation of relative transmitted dose for a step and shoot head and neck intensity modulated radiation therapy using a scanning liquid ionization chamber electronic portal imaging device. *J Med Phys.* 2012;**37**(1):14-26. doi: 10.4103/0971-6203.92716. PubMed PMID: 22363108. PubMed PMCID: PMC3283912.
16. Mohammadi M, Bezak E. Two-dimensional transmitted dose measurements using a scanning liquid ionization chamber EPID. *Phys Med Biol.* 2006;**51**(11):2971-85. doi: 10.1088/0031-9155/51/11/019. PubMed PMID: 16723778.
17. Russo M, Piermattei A, Greco F, Azario L, Orlandini L, Zucca S, et al. Step-and-Shoot IMRT by Siemens Beams: An EPID Dosimetry Verification During Treatment. *Technol Cancer Res Treat.* 2016;**15**(4):535-45. doi: 10.1177/1533034615590962. PubMed PMID: 26134437.
18. Chytyk K, McCurdy BM. Comprehensive fluence model for absolute portal dose image prediction. *Med Phys.* 2009;**36**(4):1389-98. doi: 10.1118/1.3083583. PubMed PMID: 19472646.
19. Berry SL, Sheu RD, Polvorosa CS, Wuu CS. Implementation of EPID transit dosimetry based on a through-air dosimetry algorithm. *Med Phys.*

2012;**39**(1):87-98. doi: 10.1118/1.3665249. PubMed PMID: 22225278.

20. Chen J, Chuang CF, Morin O, Aubin M, Pouliot J. Calibration of an amorphous-silicon flat panel portal imager for exit-beam dosimetry. *Med Phys.* 2006;**33**(3):584-94. doi: 10.1118/1.2168294. PubMed PMID: 16878562.
21. Chytyk-Praznik K, VanUytven E, vanBeek TA, Greer PB, McCurdy BM. Model-based prediction of portal dose images during patient treatment. *Med Phys.* 2013;**40**(3):031713. doi: 10.1118/1.4792203. PubMed PMID: 23464308.
22. Dogan N, Mijnheer BJ, Padgett K, Nalichowski A, Wu C, Nyflot MJ, et al. AAPM Task Group Report 307: Use of EPIDs for Patient-Specific IMRT and VMAT QA. *Med Phys*. 2023;**50**(8):e865-903. doi: 10.1002/mp.16536. PubMed PMID: 37384416. PubMed PMCID: PMC11230298.
23. McDermott LN, Wendling M, Van Asselen B, Stroom J, Sonke JJ, Van Herk M, et al. Clinical experience with EPID dosimetry for prostate IMRT pre-treatment dose verification. *Med Phys*. 2006;**33**(10):3921-30. doi: 10.1118/1.2230810. PubMed PMID: 17089854.
24. Fedorov A, Beichel R, Kalpathy-Cramer J, Finet J, Fillion-Robin JC, Pujol S, et al. 3D Slicer as an image computing platform for the Quantitative Imaging Network. *Magn Reson Imaging*. 2012;**30**(9):1323-41. doi: 10.1016/j.mri.2012.05.001. PubMed PMID: 22770690. PubMed PMCID: PMC3466397.
25. Saboori M. Development of a daily dosimetric control for radiation therapy using an electronic portal imaging device (EPID) [Dissertation]. Germany: Friedrich-Alexander-Universitaet Erlangen-Nuernberg (Germany); 2015.
26. Reich P, Bezak E, Mohammadi M, Fog L. The prediction of transmitted dose distributions using a 3D treatment planning system. *Australas Phys Eng Sci Med.* 2006;**29**(1):18-29. doi: 10.1007/BF03178824. PubMed PMID: 16623218.
27. Bertholet J. EPID–based Measurement of Transit Portal Dose Distributions in Radiotherapy. 2013. Available from: https://www.semanticscholar.org/paper/EPID-%E2%80%93-based-Measurement-of-Transit-Portal-Dose-in-Bertholet/cd510624f4f0aa91357f3d69bc1c99b291f09f41?utm_source=direct_link.